AD-A114 773    CONNECTICUT UNIV STORRS  DEPT OF METALLURGY            F/G 11/6
                THE FATIGUE OF POWDER METALLURGY ALLOYS.(U)
                JAN 82  A J MCEVILY                              AFOSR-81-0046
UNCLASSIFIED                                    AFOSR-TR-82-0216            NL

END
DATE
FILMED
6-82
DTIC

MICROCOPY RESOLUTION TEST CHART

③

| REPORT DOCUMENTATION PAGE | | READ INSTRUCTIONS BEFORE COMPLETING FORM |
|---|---|---|
| 1. REPORT NUMBER **AFOSR-TR. 82-0216** | 2. GOVT ACCESSION NO. AD-A444 773 | 3. RECIPIENT'S CATALOG NUMBER |
| 4. TITLE (and Subtitle) THE FATIGUE OF POWDER METALLURGY ALLOYS | | 5. TYPE OF REPORT & PERIOD COVERED Scientific ----- Annual 12/1/80 - 11/30/81 |
| | | 6. PERFORMING ORG. REPORT NUMBER |
| 7. AUTHOR(s) A. J. McEvily | | 8. CONTRACT OR GRANT NUMBER(s) AFOSR-81-0046 |
| 9. PERFORMING ORGANIZATION NAME AND ADDRESS University of Connecticut Metallurgy Dept. Storrs, CT 06268 | | 10. PROGRAM ELEMENT, PROJECT, TASK AREA & WORK UNIT NUMBERS 61102F 2306/A1 |
| 11. CONTROLLING OFFICE NAME AND ADDRESS Air Force Office of Scientific Research Bolling AFB, Building 410 Washington, D.C. 20332 | | 12. REPORT DATE January 8, 1982 |
| | | 13. NUMBER OF PAGES 24 |
| 14. MONITORING AGENCY NAME & ADDRESS(if different from Controlling Office) | | 15. SECURITY CLASS. (of this report) Unclassified |
| | | 15a. DECLASSIFICATION/DOWNGRADING SCHEDULE |

16. DISTRIBUTION STATEMENT (of this Report)

Approved for public release;
distribution unlimited.

17. DISTRIBUTION STATEMENT (of the abstract entered in Block 20, if different from Report)

18. SUPPLEMENTARY NOTES

DTIC
ELECTE
MAY 24 1982
E

19. KEY WORDS (Continue on reverse side if necessary and identify by block number)

High strength aluminum powder metallurgy alloys
Fatigue crack propagation
Crack closure
corrosion fatigue

20. ABSTRACT (Continue on reverse side if necessary and identify by block number)

Fatigue crack growth in the powder metallurgy alloys X7090-T6 and X7091-T7E69 has been studied at two R ratios (0.05 and 0.5) in air. Additional tests in a 3-1/2% NaCl environment have also been made. Particular emphasis has been placed on the study of the crack closure process on the near-threshold region. Comparisons are made with the fatigue crack growth characteristics of an ingot metallurgy product, 7075-T76. In all alloys high closure levels are observed at R=0.05 in the near threshold region, an indication that Mode II is operative.

(continue)

DD FORM 1473
1 JAN 73

82

20. At R=0.5 the closure effect is much less pronounced except at the threshold itself, an indication that Mode I is dominant. These indications of the operative crack growth modes are supported by fractographic examination. In the NaCl environment it was found that the threshold level is higher than in air as a result of the formation of corrosion products which increase the degree of closure. Further, a unique relationship between the rate of crack growth and the range of the stress intensity factor was not observed as the result of corrosion product build-up behind the crack tip.

AFOSR-TR- 82-0216

ANNUAL REPORT

on

THE FATIGUE OF POWDER METALLURGY ALLOYS

U.S. Air Force Grant No. AFOSR 81-0046

Covering Period

1 December 1980 to 30 November 1981

Submitted to

The Air Force Office of Scientific Research

AFOSR/NE
Bolling AFB
Washington, DC 20332

Attn: Dr. Alan H. Rosenstein
Program Manager

Submitted by

Professor A. J. McEvily, Jr.

Metallurgy Department U-136
University of Connecticut
Storrs, Connecticut 06268

(203)486-2941

January 1982

| Accession For | | |
|---|---|---|
| NTIS GRA&I | | ☒ |
| DTIC TAB | | ☐ |
| Unann ced | | ☐ |
| Ju. tion | | |
| By | | |
| Distribution/ | | |
| Availability Codes | | |
| Dist | Avail and/or Special | |
| A | | |

# INTRODUCTION

This report covers the first year of a program of research aimed at improving our understanding of fatigue processes in powder metallurgy (P/M) alloys of interest in structural applications. During this period attention has been focussed on fatigue crack growth characteristics of two aluminum P/M alloys, X7090 and X7091. For comparison purposes, the ingot metallurgy (I/M) alloy 7075-76 has also been tested. The results of tests in air as a function of mean stress level, and in a sodium chloride environment will be described.

## MATERIALS AND EXPERIMENTS

The alloys described in this report were obtained in extruded form from Alcoa via Lockheed-California Company. These alloys are:

    P/M X7090-T6

    P/M X7091-T7E69

    I/M 7075-T76

The nominal chemical compositions and mechanical properties for these materials are given in Table 1 and Table 2, respectively. The microstructures of the P/M alloys are shown in Figs. 1 and 2. Both microstructures and fine and uniform.

The specimens for fatigue crack growth tests were 6.3mm thick of the ASTM compact tension type with an effective width, W, of 57.2mm and a half height, H, of 34.4mm (H/W = 0.6). The specimens were machined from 1.5-inch thick plates, in eahc of the orientations L-T and T-L. Because of the extent of material removed during machining any possible residual stress effect on fatigue crack growth is thought to be minimal.

The fatigue tests were conducted at a load ratio R ($R = K_{min}/K_{max}$) of 0.05 at room temperature ($\sim$20°C) in air at a relative humidity level of 50%.

The X7090 T-L and X7091 L-T specimens were also tested at a load ratio of
0.5. In addition to the tests in air the X7091 L-T alloy was tested in
3.5% NaCl distilled water at a load ratio of 0.05. The frequency of cyclic
loading was generally 50 Hz with a sinusoidal waveshape but a slower frequency
in the range of 20 to 5 Hz was employed in the higher growth rate region
above $5 \times 10^{-5}$ mm/cycle.

To obtain a threshold value, a K-decreasing test was used. $\Delta K_{TH}$ was
determined as the stress intensity factor range, $\Delta K$, at which no crack growth
was observed for at least $2 \times 10^6$ cycles. For all specimens, once $\Delta K_{TH}$ had
been achieved the load was slightly raised and a K-increasing test was con-
ducted under constant load amplitude.

Measurements of the crack opening loads were taken using the modified
elastic compliance method in which the elastic compliance was electronically
subtracted from the total crack opening displacement (COD) signal to increase
sensitivity.

## RESULTS AND DISCUSSION

### R = 0.05 Tests

The results of fatigue crack growth tests at R = 0.05 are shown in
Fig. 3. As seen in the figure, the P/M alloys show faster growth rates in
the intermediate region as compared to the I/M 7075 alloy. At higher growth
rates the growth rate curves for the P/M alloys diverge because of a lower
fracture toughness of the X7090 alloy. No significant orientation effect
in terms of the growth rate was observed in the intermediate region of both
the P/M alloys.

In the near-threshold region, growth rates of the P/M alloys were
slower than those of the I/M alloy of the same orientation. It was also
seen that threshold levels of the P/M alloys were higher than for the I/M
7075 alloy. In contrast to a generally observed trend that an increase in

tensile strength decreases a threshold level, a similar threshold level was obtained for both the X7091 T-L and X7090 T-L alloys, although tensile and yield strengths of the 7090 alloy are higher than those of the X7091 alloy. No difference in the near threshold fatigue crack growth behavior was found in the X7090 alloy, but the significant orientation effect was observed in the X7091 alloy, i.e. the T-L direction was more resistant to the near-threshold fatigue crack growth as compared to the L-T direction.

The results of crack opening load measurements are presented in Fig. 4 in terms of the ratio of Kop to Kmax as a function of $\Delta K$ where Kop and Kmax are the stress intensity level at crack opening and the maximum stress intensity factor of cycling, respectively. This figure indicates that the crack closure effect on fatigue crack growth is very high in the near threshold region and falls to a much lower level as $\Delta K$ increases. Although all alloys tested in this study follow a similar trend, crack closure levels at a comparable $\Delta K$ level are considerably different depending upon the type of alloy. It is seen that both the X7090 L-T and T-L alloys show the greatest crack closure effect in contrast to the relatively low crack closure levels obtained in the X7091 alloy. It is noted that in the near-threshold region the X7091 T-L alloy showed more crack closure than the X7091 L-T alloy.

Fractographic analysis revealed that the fracture appearance of the X7090 alloy in the near threshold region consists of shear facets indicating that a combination of mode II and mode I crack growth is dominant in this region. Fig. 5 is a fractograph taken at a growth rate of $1 \times 10^{-6}$ mm/cycle in the X7090 T-L alloy showing examples of the shear facet. The shear facets started to appear approximately at a $\Delta K$ of 4 MPa$\sqrt{m}$ where the corresponding growth rate da/dN is $1 \times 10^{-5}$ mm/cycle. The process of crack growth takes place by the opening mode above this region. It was also

found that shear mode crack growth was increasingly dominant as $\Delta K$

approached the threshold level, resulting in higher crack closure levels

in the near-threshold region. Because of the nature of combined mode II

and mode I crack growth, extensive fretting action takes place behind the

crack tip. As a result; the fracture surface at the threshold level was

somewhat smooth as the result of errosion as shown in Fig. 6.

Fractographic analysis on the fracture surface of the X7091 alloys

revealed that the fracture appearance in the near-threshold region is also

relatively smooth without clear evidence of shear facets, as shown in Figs.

7 and 8. These fractographs were taken at a growth rate of $1 \times 10^{-6}$ mm/cycle

and contrast with the fracture appearance of the X7090 T-L alloy shown in

Fig. 5. The surface is much smoother in appearance, evidence of inte-

granular cracking is seen, and there is some type of debris present. At

the threshold level for X7091 L-T the fracture surface is rather smooth,

Fig. 9, on the X7091 alloy as compared to the X7090 alloy. Fig. 10 shows

the appearance of fatigue cracks at threshold for three types of alloys

tested. Both the X7091 L-T and X7091 T-L alloys show the presence of debris

on the specimen side surfaces. The debris moved from the specimen interior

through the crack during cycling, with the greatest amount of debris accumu-

lated at the threshold level. No debris was observed for the X7090 alloy

which shows higher crack closure levels than the X7091 alloy.

It is evident that as a result of the crack closure process in the X7091

alloy a great deal more debris is formed in this than in the case of the

other alloys studied. It is possible that this debris consists of individual

grains which have separated along relatively weak grain boundaries. We

are currently examining the nature of the grain boudnary in these alloys

to determine if either an aluminum oxide or cobalt phase is concentrated

there which might account for weaker grain boundary paths. We note that this

(Final Report to AFOSR-78-3732, Nov. 1981) has attributed grain boundary

weakness in X7091 to $Al_2O_3$ particles.

It also seems likely that as the fretted debris is extruded to the surfaces of the specimen that that extent of crack closure would decrease as observed.

## R = 0.5 Tests

Results of fatigue crack growth tests at R = 0.5 are presented in Fig. 11. As expected, a lower threshold level and higher growth rates for a given value of $\Delta K$ were obtained for both the X7090 T-L and X7091 L-T alloy as compared to those at R = 0.05. Measurements of crack opening loads were also taken in these tests. These measurements were taken without unloading below minimum load levels. The results indicated no crack closure except perhaps just at the threshold for both the alloys. Fig. 12 shows the fracture appearance of the X7090 T-L alloy observed at a growth rate of $1.0 \times 10^{-6}$ mm/cycle. It is seen from the figure that the crack path in the near-threshold region is transgranular. It should be noted that the fracture appearance in the near threshold region is relatively smooth and not particularly crystallographic. This appearance is in contrast to the tortuous fracture appearance associated with the combination of mode II and mode I crack growth commonly observed in the near threshold region for this alloy at R = 0.05 as shown in Fig. 5. In the present case, shear facets were observed only very near to the threshold as shown in Fig. 13. As yet, the significant effect of load ratio, R, on the near-threshold fatigue crack growth has not been fully understood. The present fractographic analysis clearly indicates that at R = 0.5 a mode I crack growth is dominant even in the near threshold region. As a result, there is little or no crack closure effect on the near threshold fatigue crack growth. This results in a lower threshold level as compared to that at a low R ratio.

## Corrosion Fatigue

Fig. 14 presents the result of a corrosion fatigue test for the X7091 L-T alloy in 3.5% NaCl in distilled water together with results obtained in air. In a K-decreasing test, crack growth rates in the NaCl solution were much faster than those in air in the intermediate region, but were slower in the near-threshold region. It was found that the rate of crack growth gradually decreased with continued cycling at a $\Delta K$ of 2.2 MPa$\sqrt{m}$. The crack was finally self-arrested at this $\Delta K$ level, resulting in a higher $\Delta K_{TH}$ level than that in air. Paris et. al., [1] reported a similar result obtained for a A533 steel i.e. a threshold level in distilled water is higher than in air, and suggested that this higher threshold level in distilled water is due to corrosion products formed between the mating fracture surfaces which significantly reduce the effective crack tip opening displacement. Ritchie et. al.[2] and Stewart [3] have further advanced the effect of corrosion products on the near-threshold crack growth in laboratory air and inert gas environments. In the present study, as seen in Fig. (15) crack closure levels in the near-threshold region are much higher in the NaCl solution than in air where the combination of mode II and mode I crack growth controls the crack closure behavior. It is apparent from the figure that in the NaCl environment the effect of corrosion products on crack closure behavior is much greater than that of the mode-II and mode I crack growth.

In air tests K decreasing test results generally agree with those obtained by a K-increasing test. However, in the present corrosion fatigue test much slower crack growth rates were obtained in the K increasing test than in the K-decreasing test. Since the specimen for the K increasing test had been exposed to the NaCl environment for approximately three days, it is thought that the difference in growth rate is attributed to the

presence of thick corrosion products. This result indicates that in the present case a threshold value and growth rates in the near-threshold region are predominantly controlled by the thickness of corrosion products.

References

1.  Paris, P. C., et. al., ASTM STP 513, 1972, p. 141.

2.  Suresh, S., Zamiski, G. F., and Ritchie, R. O., Metallurgical Trans. A, Vol. 12A, 1981, p. 1435.

3.  Stewart, A. T., Engineering Fracture Mechanics. Vol. 13, 1980, p. 463.

## Papers Submitted

1. K. Minakawa and A.J. McEvily, On Near-Threshold Fatigue Crack Grwoth in Steels and Aluminum Alloys, presented at the International Symposium on Fatigue Thresholds, Stockholm, June 1981.

2. K. Minakawa and A.J. McEvily, On Crack Closure in the Near-Threshold Region, Scripta Metallurgica, Vol. 15, p. 633, 1981.

3. A.J. McEvily and K. Minakawa, Recent Developments in Fatigue Crack Growth, presented at the U.S.-Japan Joint Seminar, "Fracture Tolerance Evaluation" Honolulu, Hawaii, December, 1981.

## Papers in Preparation

1. A.J. McEvily, On the Quantitative Analysis of Fatigue Crack Propagation, to be presented at the Int. Conf. on Quantitative Measurement of Fatigue Damage, ASTM, May 1982, Dearborn, Michigan.

2. A.J. McEvily and K. Minakawa, On Mixed Mode Effect in Fatigue Crack Propagation, Second U.S.-Greece Seminar on Mixed Mode Fracture and Fatigue, March 1982, Lehigh University.

3. K. Minakawa, J.A. Ruppen and A.J. McEvily, On Fatigue Crack Growth in Aluminum Alloys and Titanium Alloys in the Near-Threshold Region, to be presented at the Symposium on Fractography in Failure Analysis of Ceramics and Metals, ASTM, April 1982, Philadelphia, Penn.

## Personnel

| | |
|---|---|
| Principal Investigator: | A. J. McEvily |
| Post-Doctoral Research Associate: | K. Minakawa |
| Research Technician: | R. Shover |
| Ph.D. Candidates: | J. A. Ruppen |
| | C. Hoffmann (PhD to be awarded in May 1982) |
| Students: | Greg Levan |
| | Paul Inguanti |
| | Mark Hayden |

Fig. 1   –   Microstructure of extruded P/M X7090.
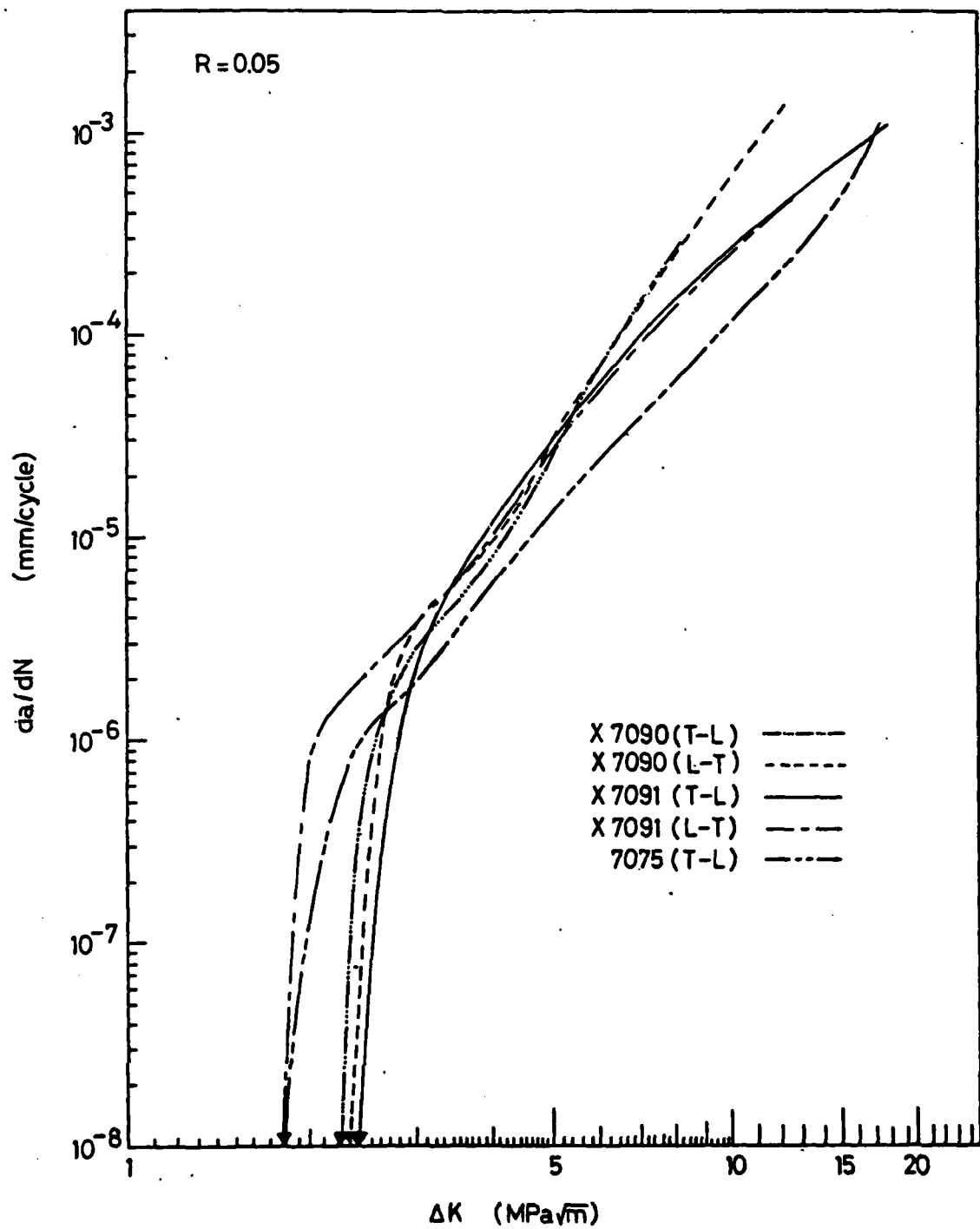
Fig. 2   –   Microstructure of extruded P/M X7091.

Fig. 3   –   Fatigue crack growth rates as a function of $\Delta K$ for P/M and
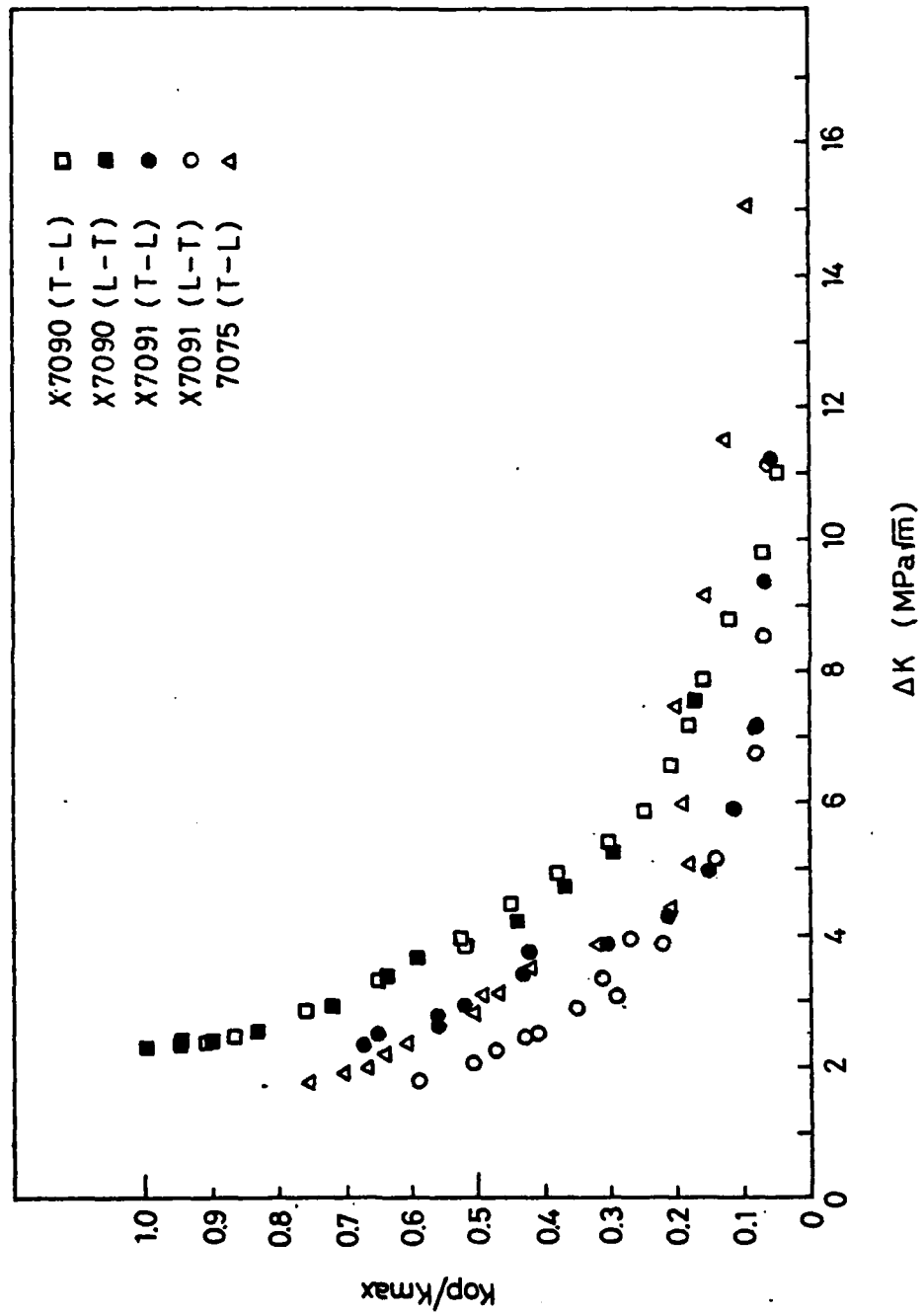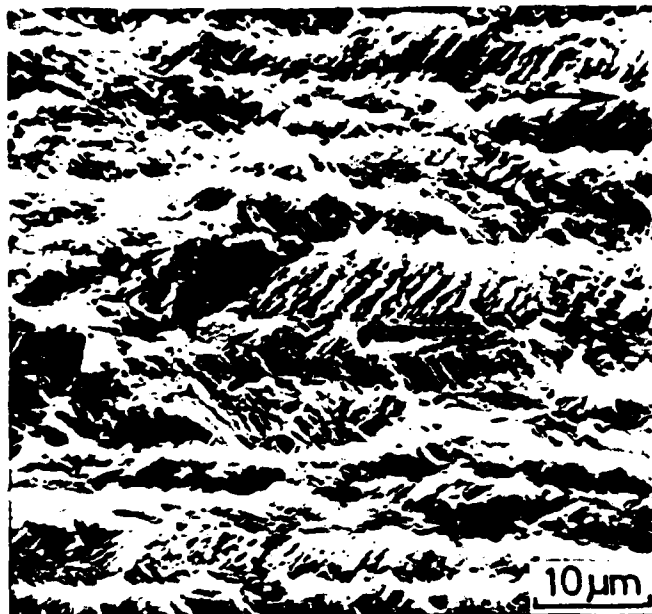I/M alloys (R = 0.05).

Fig. 4   –   Ratio of Kop to Kmax as a function of $\Delta K$ for P/M and I/M alloys.

Fig. 5   –   Fracture surface of X7090 T-L alloy.

Fig. 6   –   Fracture surface of X7090 alloy at threshold.

Fig. 7   –   Fracture surface of X7091 alloy.

Fig. 8   –   Fracture surface of X7091 alloy showing oxide debris.

Fig. 9   –   Fracture surface of X7091 at threshold. Vertical arrow indicates
position of crack front at threshold.

Fig. 10 –   A specimen of crack tip region at free surface at threshold.

Fig. 11 –   Fatigue crack growth rates as a function of $\Delta K$ for P/M alloys
(R = 0.5).

Fig. 12 –   Fracture surface of X7090 at R = 0.5.

Fig. 13 –   Fracture surface of X7090 at R = 0.5 near threshold.

Fig. 14 –   Rate of fatigue crack growth in 3.5% NaCl for X7091 (L-T)
compared to growth rate in air under decreasing and increasing
$\Delta K$ conditions.

Fig. 15 –   Ratio of Kop to Kmax as a function of $\Delta K$ for X7091 in air and
in 3.5% NaCl solution.

## Table 1.    Nominal Chemical Compositions (wt%)

| | Cu | Mg | Mn | Si | Fe | Co | Zn | Ti | Cr |
|---|---|---|---|---|---|---|---|---|---|
| X7090 (MA67, CT90) | 0.60-1.30 | 2.00-3.00 | | max0.12 | max0.15 | 1.00-1.90 | 7.30-8.70 | | |
| X7091 (MA87 CT91) | 1.20-2.00 | 2.20-3.00 | | max0.15 | max0.20 | 0.20-0.60 | 6.00-7.00 | | |
| 7075 | 1.20-2.00 | 2.10-2.90 | max0.30 | max0.40 | max0.50 | | 5.10-6.10 | max0.20 | 0.18-0.28 |

## Table 2.    Mechanical Properties

| | Orientation | $\sigma_{ys}$(MPa) | UTS(MPa) | Elongation(%) |
|---|---|---|---|---|
| X7090 (T6) | L | 650 | 683 | 8.5 |
| | T | 580 | 634 | 8.2 |
| X7091 (T7E69) | L | 544 | 593 | 13 |
| | T | 527 | 580 | 12 |
| 7075 (T76) | L | 471 | 540 | 7 |
| | T | 420 | 461 | 6 |
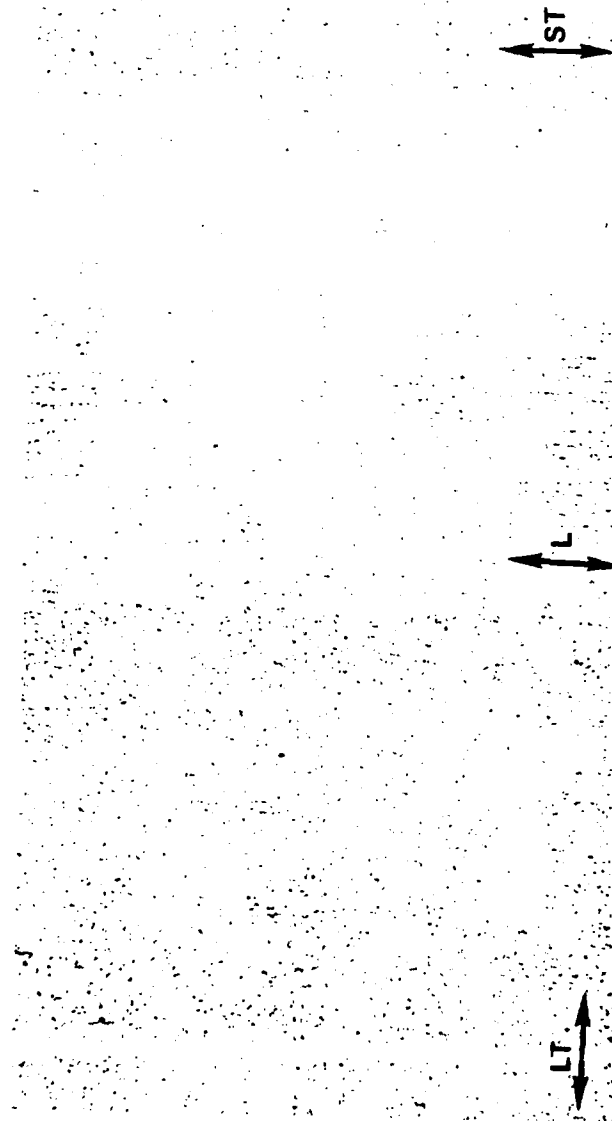
X 7090

40 μm

Fig. 1 – Microstructure of extruded P/M X7090.

Fig. 2 -- Microstructure of extruded P/M X7091.

Fig. 3 – Fatigue crack growth rates as a function of ΔK for P/M and I/M alloys (R = 0.05).

Fig. 4 – Ratio of Kop to Kmax as a function of ΔK for P/M and I/M alloys.

X7090 T-L      $1 \times 10^{-6}$ mm/cycle

Fig. 5 - Fracture surface of X7090 T-L alloy.
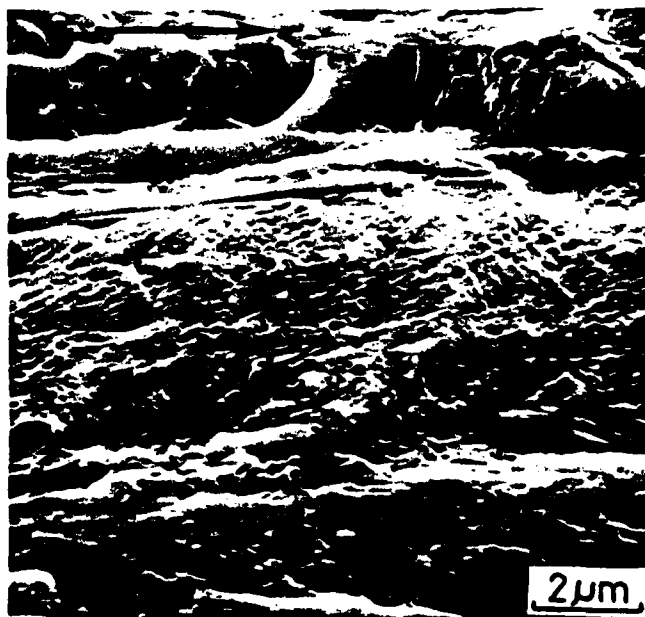


X7090 T-L      $\Delta K_{TH}$
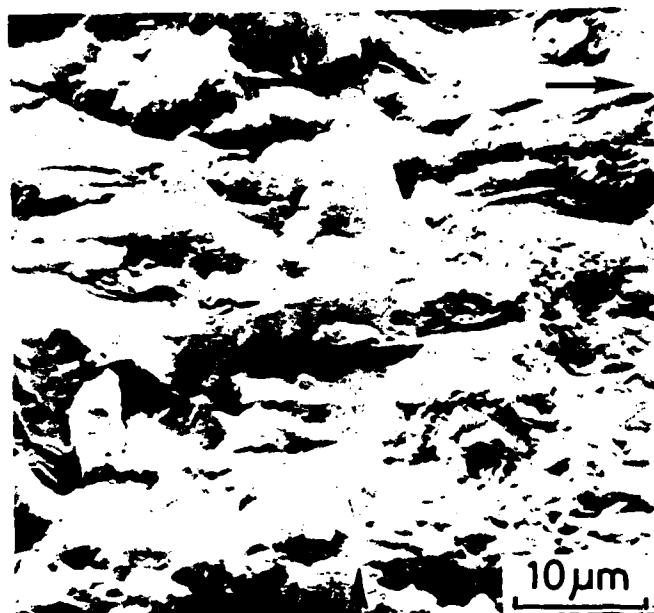
Fig. 6 - Fracture surface of X7090 alloy at threshold.
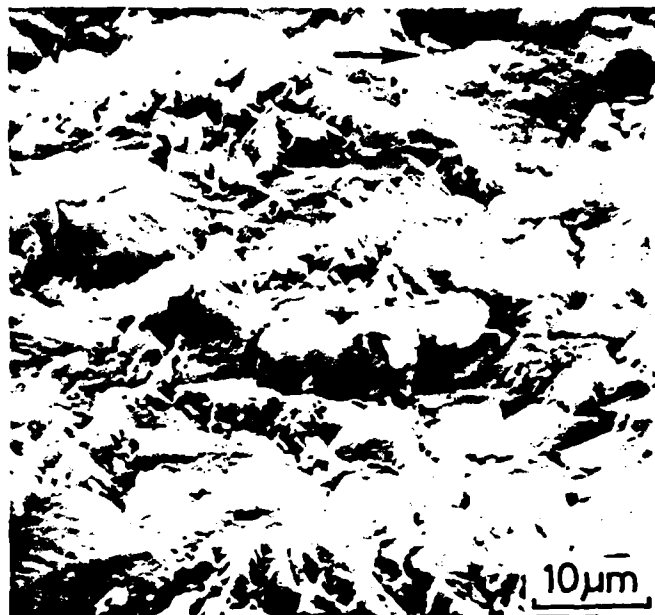
X7091 L-T     $1 \times 10^{-6}$ mm/cycle

Fig. 7 - Fracture surface of X7091 alloy.
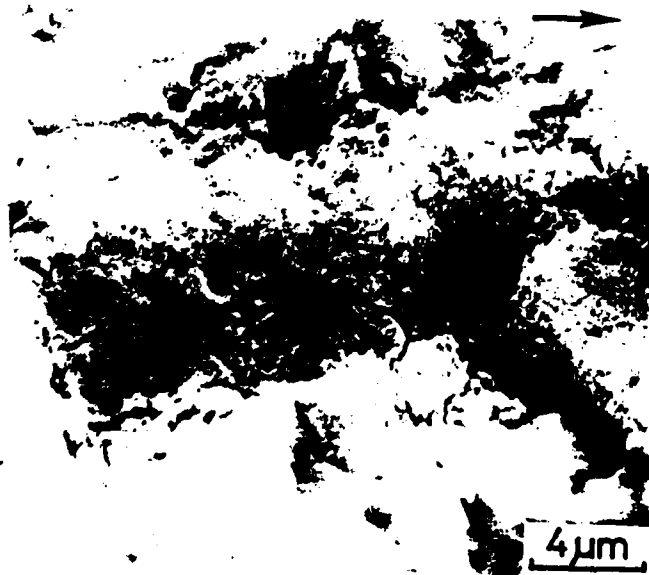


X7091 T-L     $1 \times 10^{-6}$ mm/cycle

Fig. 8 - Fracture surface of X7091 alloy showing oxide debris.

X7091 L-T    $\Delta K_{TH}$

Fig. 9 – Fracture surface of X7091 at threshold.  Vertical arrow indicates position of crack front at threshold.

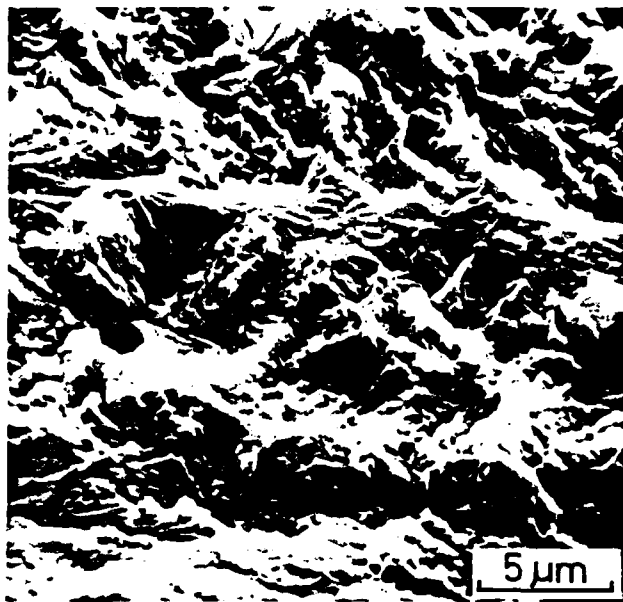Fig. 10 – A specimen of crack tip region at free surface at threshold.
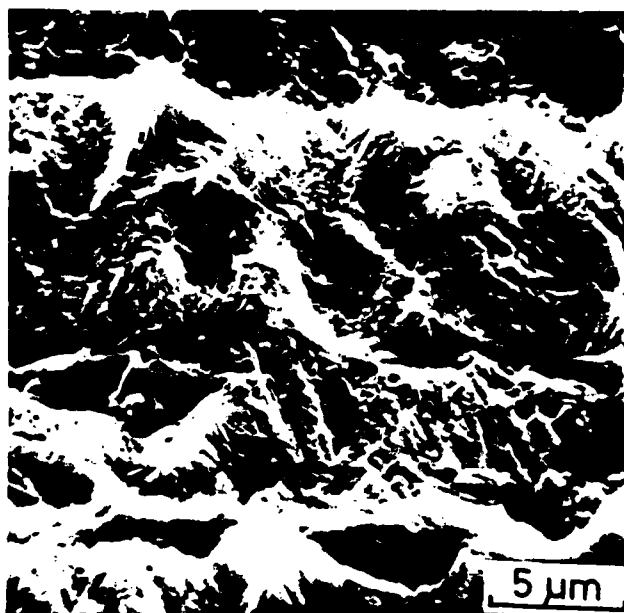
Fig. 11 – Fatigue crack growth rates as a function of ΔK for P/M alloys (R = 0.5).

X7090 T-L      $1 \times 10^{-5}$ mm/cycle

Fig. 12 – Fracture surface of X7090 at R = 0.5.



X7090 T-L      $2 \times 10^{-7}$ mm/cycle

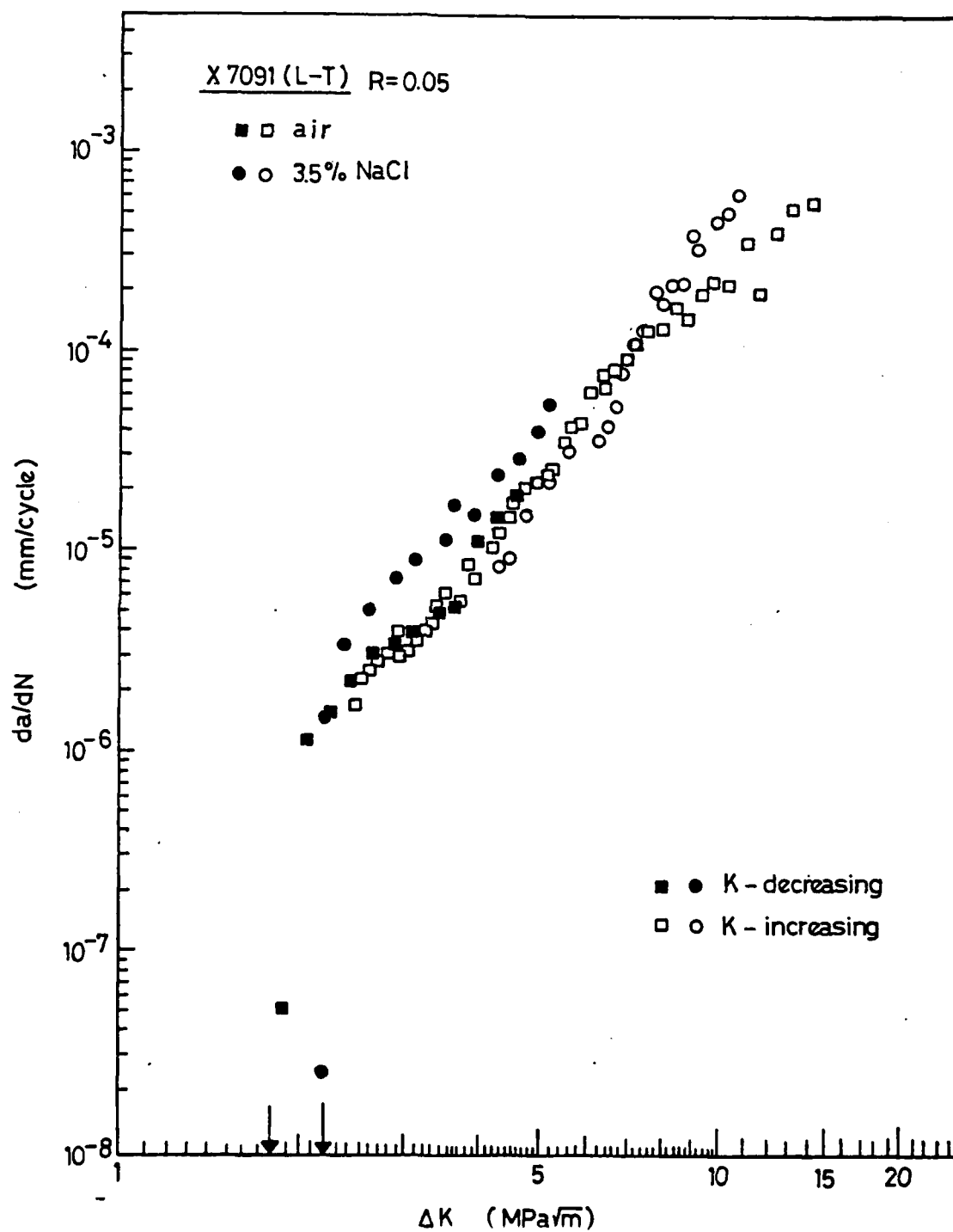Fig. 13 – Fracture surface of X7090 at R = 0.5 near threshold.

Fig. 14 - Rate of fatigue crack growth in 3.5% NaCl for X7091 (L-T) compared to growth rate in air under decreasing and increasing K conditions.
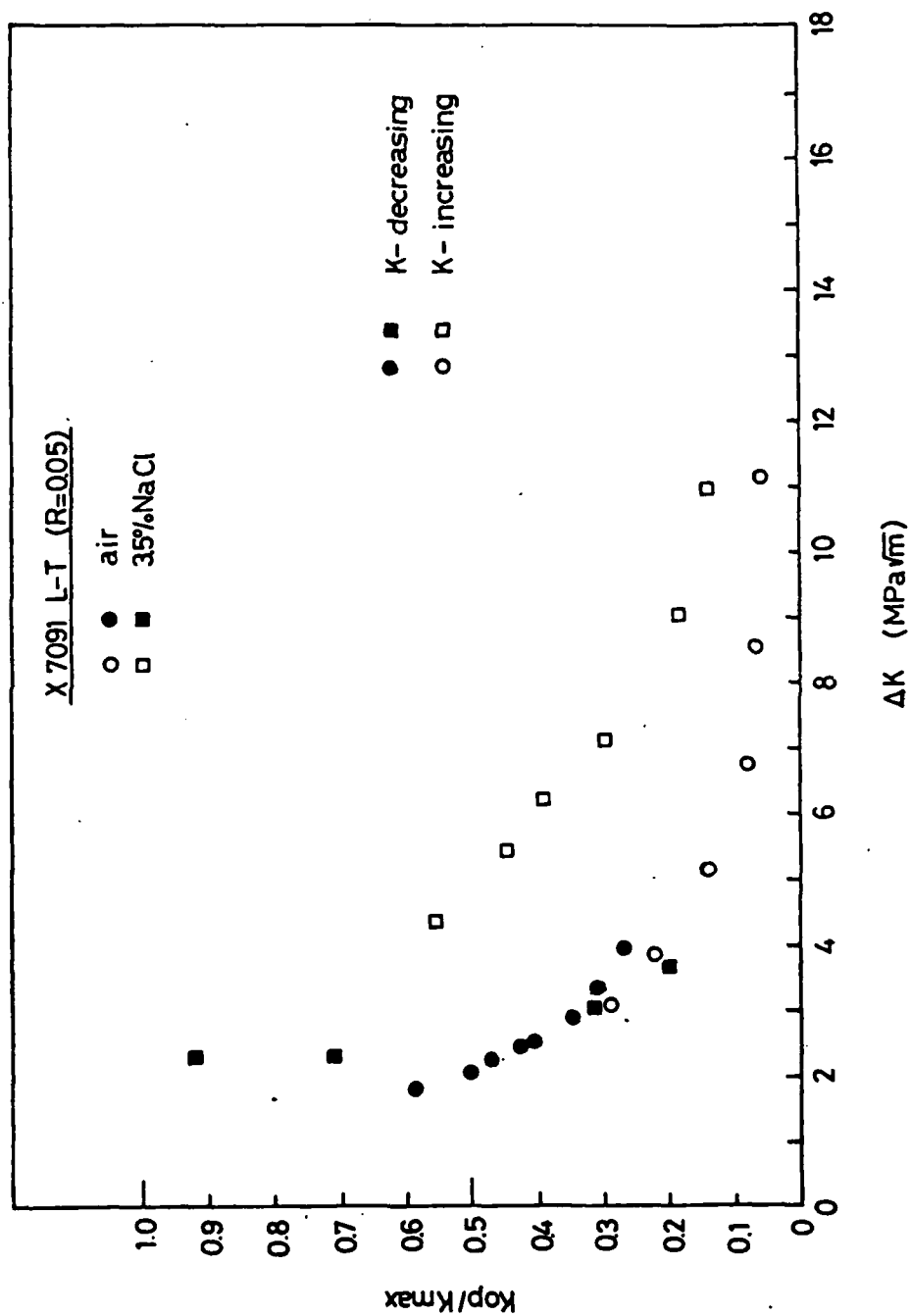
Fig. 15 – Ratio of Kop to Kmax as a function of ΔK for X7091 in air and in 3.5% NaCl solution.